bioRxiv preprint doi: https://doi.org/10.1101/157503; this version posted June 29, 2017. The copyright holder for this preprint (which was not certified by peer review) is the author/funder. All rights reserved. No reuse allowed without permission.

## Title

# Antidiabetic drugs "gliptins" affect biofilm formation by the cariogenic bacterium *Streptococcus mutans* through inhibition of the bacterial DPP IV-like enzyme.

## Authors

Arpan De[1], Arianna Pompilio[2,3], Jenifer Francis[4], Iain C. Sutcliffe[4], Gary W. Black[4], Giulio Lupidi[1], Dezemona Petrelli[5], Luca A. Vitali[1]*

**Authors' affiliation**

1. School of Pharmacy, University of Camerino, Camerino, Italy.
2. Department of Medical, Oral and Biotechnological Sciences, School of Medicine, "G. d'Annunzio" University of Chieti-Pescara
3. Center of Excellence on Ageing, "G. d'Annunzio" University Foundation, Chieti.
4. Department of Applied Sciences, Faculty of Health & Life Sciences, Northumbria University, Newcastle upon Tyne, UK
5. School of Biosciences and Veterinary Medicine, University of Camerino, Camerino, Italy.

**Corresponding Author**

Vitali Luca Agostino
ph. +39-0737-403282, fax +39-0737-403281, Email: luca.vitali@unicam.it

**Keywords**

Gliptins, *Streptococcus mutans*, Biofilm, X-prolyl dipeptidyl peptidase

**Subject Category**

Physiology and metabolism

**Word Count**: 6037

**Abbreviations:**

XPDAP: X-prolyl dipeptidyl peptidase, DPP IV: Dipeptidyl peptidase IV, AHD: anti-human DPP IV drugs.

bioRxiv preprint doi: https://doi.org/10.1101/157503; this version posted June 29, 2017. The copyright holder for this preprint (which was not certified by peer review) is the author/funder. All rights reserved. No reuse allowed without permission.


## Abstract

*Streptococcus mutans*, a dental caries causing odontopathogen, produces X-prolyl dipeptidyl peptidase (Sm-XPDAP, encoded by *pepX*), a narrow range serine protease known to have a nutritional role. Considering the potential of proteases as therapeutic targets in pathogens, this study was primarily aimed at investigating the role of Sm-XPDAP in contributing to virulence-related traits. Dipeptidyl peptidase (DPP IV), an XPDAP analogous enzyme found in mammalian tissues, is a well known therapeutic target in Type II diabetes. Based on the hypothesis that gliptins, commonly used as anti-human-DPP IV drugs, may affect bacterial growth upon inhibition of Sm-XPDAP, we have determined their *ex vivo* antimicrobial and anti-biofilm activity towards *S. mutans*. All three DPP IV drugs tested reduced biofilm formation as determined by crystal violet staining. In order to link the observed biofilm inhibition to the human-DPP IV analogue present in *S. mutans* UA159, a *pepX* isogenic mutant was generated. In addition to reduced biofilm formation, CLSM studies of the biofilm formed by the *pepX* isogenic mutant showed these were comparable to those formed in the presence of saxagliptin, suggesting a probable role of this enzyme in biofilm formation by *S. mutans* UA159. The effects of both *pepX* deletion and DPP IV drugs on the proteome were studied using LC-MS/MS. Overall, this study highlights the potential of Sm-XPDAP as a novel anti-biofilm target and suggests a template molecule to synthesize lead compounds effective against this enzyme.

bioRxiv preprint doi: https://doi.org/10.1101/157503; this version posted June 29, 2017. The copyright holder for this preprint (which was not certified by peer review) is the author/funder. All rights reserved. No reuse allowed without permission.

## Introduction

Dental caries is the most prevalent, multifactorial, globally increasing oral health problem among children and adults (Bagramian *et al.*, 2009; Selwitz *et al.*, 2007). It is a manifestation of biofilm formation by members of the indigenous oral microbiota, mainly *Streptococcus mutans*, *Streptococcus sobrinus* and lactobacilli. The *S. mutans* genome codes for several peptidases (Ajdić *et al.*, 2002). Evidence has also been presented that exoglycosidase and endopeptidase expression allows utilization of glycoprotein and anionic polypeptides in human saliva as a source of nutrition (Cowman *et al.*, 1977, 1975; Smith & Beighton, 1986). Based on previous reports, the essentiality of oligopeptide transport in *S. mutans*, as well as an abundance of lipoprotein-based amino acid uptake systems encoded in its genome, further supports the presumed importance of these peptidases in metabolism (Ajdić *et al.*, 2002; Cowman & Baron, 1990). X-prolyl dipeptidyl aminopeptidase (XPDAP) is a narrow substrate range cytoplasmic endopeptidase which may help in the utilization of proline rich salivary polypeptides in *S. mutans* (Cowman & Baron, 1993, 1997). Previously described collagenolytic and caseinolytic activities may further suggest the importance of XPDAP as a putative virulence factor and nutritional necessity in *S. mutans* (Cowman *et al.*, 1975; Rosengren & Winblad, 1976).

An analogous enzyme to XPDAP, DPP IV is also found in mammalian tissues and is a potential target for maintaining glucose homeostasis in Type II diabetic patients (Cowman & Baron, 1997; Green *et al.*, 2006). Diabetes, an abnormal metabolic disorder, is an epidemic of significant healthcare concern among both developed and developing countries (King *et al.*, 1998). Certain drugs, namely saxagliptin, vildagliptin and sitagliptin, are commonly used anti-human DPP IV (AHD) molecules used in the treatment of Type II diabetes(Green *et al.*, 2006). DPP IV targets incretin hormones such as GLP-1, thereby decreasing their plasma levels. Inhibition of DPP IV

bioRxiv preprint doi: https://doi.org/10.1101/157503; this version posted June 29, 2017. The copyright holder for this preprint (which was not certified by peer review) is the author/funder. All rights reserved. No reuse allowed without permission.

leads to the opposite effect, which results in a stimulation of insulin secretion from the pancreas and a restoration of glucose homeostasis in diabetic patients (Wang *et al.*, 2012).

Previous studies have reported a role of XPDAP in virulence of bacteria. For example, extracellular XPDAP present in *Streptococcus suis* and *Streptococcus gordonii* was found to have a role in cellular invasion (Ge *et al.*, 2009; Goldstein *et al.*, 2001), while deficiency of XPDAP in the periodontal pathogen *Porphyromonas gingivalis* caused altered virulence, through lesser connective tissue destruction and less effective mobilization of inflammatory cells in a mouse abscess model (Yagishita *et al.*, 2001). As a novel approach, our recent investigation on inhibition of *S. mutans* XPDAP (Sm-XPDAP, encoded by *pepX*) by AHD molecules has found significant inhibition by saxagliptin *in vitro* (De *et al.*, 2016). In an extension of this work and hypothesising a probable role of Sm-XPDAP in virulence, we have here evaluated the *ex vivo* effect of these molecules on cell growth and biofilm formation by *S. mutans*. In order to link the observed effect to the inhibition of Sm-XPDAP, a *pepX* (SMU.35) isogenic mutant was generated. Furthermore, whole cell proteome analysis of AHD treated cells and the isogenic mutant was performed to identify possible consequences of Sm-XPDAP inhibition or deletion.

## Methods

### Microorganisms and growth conditions

*S .mutans* UA159 (ATCC 700610) was used for protein purification and cloning purposes. Glycerol stocks of *S. mutans* UA159 were used to grow overnight cultures in Brain Heart Infusion broth (BHI). All the incubations of *S. mutans* cultures were done at 37$^{o}$C under 5% $CO_2$ atmosphere (Cowman & Baron, 1990).

bioRxiv preprint doi: https://doi.org/10.1101/157503; this version posted June 29, 2017. The copyright holder for this preprint (which was not certified by peer review) is the author/funder. All rights reserved. No reuse allowed without permission.

Minimum Inhibitory Concentration (MIC) and growth curves were determined in BHI broth, whereas the biofilm formation assay was evaluated in a semi-defined biofilm medium (SDM) supplemented with 20mM glucose or sucrose as described previously (Supplementary text 2) (Ahn *et al.*, 2008).

**MIC and Biofilm formation assay**

The MIC was determined by microdilution assay according to the Clinical and Laboratory Standards Institute (CLSI, 2011), with the exception of the medium used, which was BHI (Ahn *et al.*, 2012; da Silva *et al.*, 2013). Briefly an overnight culture of *S. mutans* was used to grow a fresh batch of cells till the mid-exponential phase ($O.D_{600}$ = 0.5) and added to a 96 well microtiter plate to a final concentration of 1 X $10^6$ CFU/mL. In order to determine the MIC, the highest concentration of 2048 µg/mL was serially diluted down to 4µg/mL of each AHD used. The drugs were dissolved in sterile water and an erythromycin standard was used as a positive control.

Biofilm formation was assessed by a semi-quantitative crystal violet method in polystyrene 96-well (flat bottom) cell culture plates (Costar 3595; Corning Inc., NY) as previously described (Ahn *et al.*, 2008). An overnight culture of *S. mutans* was transferred into pre-warmed BHI and grown till mid-exponential phase and then diluted 50 fold in SDM. Aliquots (100µL) of this culture were added to serially diluted drug in water (2048 µg/mL to 4µg/mL), to make a final volume of 200µL (with 100-fold final dilution of cells) and incubated for 20 hours. The culture medium was decanted and the wells were washed three times with saline (0.9% NaCl) with subsequent staining with 200 µL of 1% crystal violet for 15 minutes. In order to wash excess stain, the stained wells were washed twice with saline. The bound dye was extracted from the

bioRxiv preprint doi: https://doi.org/10.1101/157503; this version posted June 29, 2017. The copyright holder for this preprint (which was not certified by peer review) is the author/funder. All rights reserved. No reuse allowed without permission.

adherent cells using 200 µL of 99% ethanol and quantified at 495nm. The statistical analysis was performed in GraphPad Prism (v 5.0). The viability of the cells in the culture medium (planktonic phase over the formed biofilm) at each concentration of drug was determined by CFU counting.

**Construction of pepX deletion mutants**

A *pepX* deletion mutant was generated by a PCR ligation mutagenesis method (Lau *et al.*, 2002). Briefly, an erythromycin cassette was amplified using primers Ery-pOMZ291-F and Ery-pOMZ291-R harbouring NcoI/SacI restriction sites from plasmid pOMZ291 (van der Ploeg, 2008). Upstream and downstream flanking regions (about 600bps) of *pepX* were amplified using two pairs of primers, pepX-Up-F/R and pepX-Dn-F/R (Table 2). Subsequently, amplicons with similar restriction sites (either NcoI/SacI at the terminus) were digested and subjected to bipartite ligation with the erythromycin cassette separately at 16$^{o}$C overnight. The resulting ligation mixes were used for PCR to obtain a mutagenic construct using primers pepX-Up-F and pepX-Dn-R. This fragment was naturally transformed into mid log phase *S. mutans* UA159, grown in Todd-Hewitt broth containing 10% sucrose and the recombinants were selected on BHI agar containing 10µg/mL erythromycin (Petersen & Scheie, 2000).

**CLSM examination of Biofilm**

The fluorescence study of the texture of biofilms of the *pepX* mutant and wild type *S. mutans*, grown on polystyrene discs in the presence of SDM and glucose and AHD drugs as stated above, was performed using a LSM 510 META laser scanning microscope attached to an Axioplan II microscope (Zeiss). The non-adherent cells were washed in saline, biofilms were stained with Live/Dead BacLight (1X) (Molecular Probes Inc.) for 20 minutes and rinsed three times in saline

bioRxiv preprint doi: https://doi.org/10.1101/157503; this version posted June 29, 2017. The copyright holder for this preprint (which was not certified by peer review) is the author/funder. All rights reserved. No reuse allowed without permission.

to remove excess stain. Subsequently, the stained discs were examined under alpha Pan-Fluar 100X objective at an excitation wavelength of 488nm (Argon laser), and 543nm (He-Ne-laser) and emission filter ranging 585-615nm and 505-530nm for Propidium iodide and SYTO9 respectively. A series of images were acquired on x-y focal plane at different microscopic fields, while the z-stack of multidimensional complex biofilm was obtained at different depths only with the mutant and wild type. ImageJ 1.48v (NIH, USA) was used to process and enhance image quality and remodelled in Amira Trial Ver. 5.6. The proportion of viable cells (green) versus dead cells (red) was determined based on the intensity at each pixel using ImageJ (Nance *et al.*, 2013). The proportion of green signal and red signal was calculated by multiplying the total number of pixels with the given intensity (0 -255) at each channel, and then dividing it by the sum of the intensity value for each signal measured at each image stack.

**Cell Aggregation and Hydrophobicity assay**

*S. mutans* wild type and Δ*pepX* mutant, grown from an overnight culture till mid-exponential phase ($O.D_{600}$ = 0.5) in BHI, were harvested by centrifugation at 4000 rpm for 15 min. The cell pellets were washed twice with saline (0.9% NaCl). The aggregation abilities of the re-suspended cells were assessed using 5µL 0.1M $CaCl_2$, in a temperature controlled multicuvette positioner spectrophotometer (Cary 100) at 37°C for 120 min as described previously (Ahn *et al.*, 2009)

The reduction in hydrophobicity of the Δ*pepX* mutant was measured by comparing the percentage of affinity of the cells to toluene. Cells grown till mid-exponential phase were harvested, washed and resuspended in saline to obtain a cell density of 0.3 at 600nm. 250µL toluene was added into 3mL of cell suspension, vortexed and allowed to rest for 10 min at room temperature. The % of partitioned cells was calculated as described before (Ahn *et al.*, 2009) . Both the assays were performed in two biological replicates.

bioRxiv preprint doi: https://doi.org/10.1101/157503; this version posted June 29, 2017. The copyright holder for this preprint (which was not certified by peer review) is the author/funder. All rights reserved. No reuse allowed without permission.

**Evaluation of oxidative and acid stress on the mutant**

The acid tolerance level of the *pepX* mutant was compared by challenging the cells in acidic pH. *S. mutans* wild type and Δ*pepX* grown till $OD_{600}$ of 0.3 were harvested at 4000×g for 10 min at 4°C. The cells were washed in 0.1M glycine buffer (pH 7.5). The cell pellet was resuspended in glycine buffer (pH 7.5) and half of the volume of cells was centrifuged and resuspended in glycine buffer (pH 2.8). An aliquot (50-100µL) of cells from the acidic suspension and neutral suspension at different time points (0, 10, 20, 30 and 35 min) were spread plated on BHI agar. The plates were incubated at 37°C, 5% $CO_2$ for 48 hours and then the colonies counted. The plating for each dilution was done in duplicates and the effect was assessed in two independent experiments for each of the strains.

Oxidative stress tolerance of the Δ*pepX* mutant strain was assessed with a hydrogen peroxide challenge. The strains were grown in BHI at 37°C, 5% $CO_2$ till OD 0.3 and then harvested. The cell pellets were washed in 0.1M glycine buffer (pH 7.5) and resuspended in one-fifth volume of the same buffer. Half a volume of cells was centrifuged and resuspended in the same volume of buffer containing 0.2% $H_2O_2$. This step was performed in order to have essentially the same batch of cells with comparable cell density prior or post challenge with hydrogen peroxide. At various time points (0, 10, 20 and 30 min) the oxidizing activity of peroxide was stopped by adding 20µL of 5 mg/mL catalase to the treated cells and spread on BHI agar at various dilutions. In order to compare the effect, an aliquot of cell suspension was also spread plate before addition of hydrogen peroxide. All the platings at each dilution were done in duplicate and incubated at 37°C, 5% $CO_2$ for 48 hours. Two independent experiments were conducted to confirm the results.

bioRxiv preprint doi: https://doi.org/10.1101/157503; this version posted June 29, 2017. The copyright holder for this preprint (which was not certified by peer review) is the author/funder. All rights reserved. No reuse allowed without permission.

## Proteome analysis of biofilm grown cells

### *Protein isolation and pre-fractionation*

The proteome of biofilm grown cells, either in absence or presence of an AHD drug, and that of the Δ*pepX* mutant were analysed from 48mL of culture. The biofilm for each condition was set up in a 24 well cell culture plate (Greiner Bio-one, CELLSTAR) as described above. After 20 hours of incubation the planktonic phase was removed and the attached biofilm was disrupted using sterile water. The harvested cells were pooled and washed twice in PBS (1X), resuspended in lysis buffer and sonicated at 12000 – 13000 microns amplitude for 2 minutes with an intermittent 10 sec on and 10 sec off in ice. Subsequently, the cell free extract was collected by centrifugation at 14000 × g for 45 min at 4°C and acetone precipitated at -20°C overnight. The precipitated proteins were collected by centrifugation, washed in 80% and 40% acetone successively, air dried for 1 hour at room temperature and stored at -20°C for further use. The pellet was dissolved in 30mM Tris buffer (pH 8) and then partially pre-fractionated by 1D PAGE. A similar amount of calculated protein (µg) as estimated by Bradford assay, representing samples at each condition, was boiled with 5µL of loading dye for 15 min and electrophoresed at 200V for about 1 hr. The gel was stained in Coomassie Blue for 15 min followed by destaining overnight at room temperature.

### *Sample preparation and Mass spectrometry*

The protein containing gel was sectioned into pieces and then treated twice with 100mM $NH_4HCO_3$ and acetonitrile (ACN) with shaking for 30 min allowing removal of the Coomassie stain. The gel slices were then dehydrated in ACN at room temperature for 60 min, air dried for 15 min and pre-incubated in 40µg/mL trypsin (Trypsin Gold, MS Grade, Promega) at 37°C for 1

bioRxiv preprint doi: https://doi.org/10.1101/157503; this version posted June 29, 2017. The copyright holder for this preprint (which was not certified by peer review) is the author/funder. All rights reserved. No reuse allowed without permission.

hour in a water-bath. Subsequently, the gel pieces were immersed in $NH_4HCO_3$ and incubated further at 37°C overnight. On the following day, the digestion was stopped by adding 50% ACN (v/v) and 5% formic acid (v/v) with shaking for 30 min. The digested extract containing peptides was removed and transferred into a fresh vial (Fraction A). The gel pieces were further extracted using 83% ACN (v/v) and 0.2% formic acid under the same conditions (Fraction B). All the extracts containing digested peptides were then pooled (Fraction A + Fraction B) and frozen at -80°C for more than an hour. Frozen peptide digests were freeze-dried for 20- 24 hours (Alpha 1-2 LoPlus CHRIST attached to JAVAC High Vacuum pump). The samples were stored at -80°C until injection into the LC-MS/MS. Before injection, the lyophilized peptide digest was mixed in 5% ACN and 0.1% formic acid (v/v) and then run in a LC- NanoPump coupled to a tandem mass spectrometer (Thermo Q Exactive attached to HPLC Ultimate 3000 RSLC nano system), through an Easy Spray C18 column (PepMap RSLC, 75µm × 500mm, Thermo Scientific) equipped with Electro Spray Ionization, in a gradient solvent mixture of water and ACN containing 0.1% formic acid. The run was carried out for 215 minutes at a flow rate of 0.3µL/min with a scan range of 350 – 1800 m/z.

*Identification of the peptides*

The mass spectrum data (MS and $MS^2$) obtained for each set of conditions was then processed in Progenesis LC-MS v4.1. The statistically validated peptides (>2 fold change in expression and features significantly present in all of the three technical replicates, $p < 0.05$) were exported into MASCOT database for identification (Matrix Science, www.matrix-science.com). The database search was performed for MS/MS spectra of all selected peptides with carbamidomethyl and oxidised methionine as modifications, and peptide mass tolerance of ±20 ppm. After identification, peptides were imported back into Progenesis for refining for only those protein

bioRxiv preprint doi: https://doi.org/10.1101/157503; this version posted June 29, 2017. The copyright holder for this preprint (which was not certified by peer review) is the author/funder. All rights reserved. No reuse allowed without permission.

matches from *S. mutans*, reviewing and removing all the proteins with conflict, grouping all the peptides with similar protein labels, quantifying abundance level of proteins and producing a compiled report on the differential level of proteins at different conditions. To ensure robust protein identification, only those proteins consistently detected in both biological replicates, typically with a minimum of >1 peptide per protein in each run, were retained for further analysis.

**Statistical analysis**

Statistical analysis was performed using the software Statgraphics Centurion ver. XV (Statpoint Technologies, Inc., Virginia, USA). Fitting of data was done using Origin ver. 8.1 (Origin Lab Corporation, MA, USA). Inhibition of biofilm formation data were fitted using a dose/response function (Boltzmann), according to the following equation (1):

$$y = A2 + \frac{A1 - A2}{1 + e^{(x - EC50)/dx}} \qquad (1)$$

where A2 and A1 are the maximum and minimum level of biofilm formed, respectively, and $EC_{50}$ is the concentration of the drug affecting 50% biofilm formation. $EC_{50}$ values from the four replicates of the same drug were derived from the above equation and their mean calculated. Distribution of $EC_{50}$ values of the same drug were checked for normality. Analysis of variance (ANOVA) test was run to compare means from different drugs and to check variance. Probability value threshold was set to 0.05. Multiple comparison analysis was performed between pairs of data sets (considered as independent), corresponding to biofilm formation level

bioRxiv preprint doi: https://doi.org/10.1101/157503; this version posted June 29, 2017. The copyright holder for this preprint (which was not certified by peer review) is the author/funder. All rights reserved. No reuse allowed without permission.

($OD_{490nm}$) at each and every concentration of the given drug. F-test (ANOVA) was used to test for the rejection of the null hypothesis ($P < 0.05$).

bioRxiv preprint doi: https://doi.org/10.1101/157503; this version posted June 29, 2017. The copyright holder for this preprint (which was not certified by peer review) is the author/funder. All rights reserved. No reuse allowed without permission.

## Results

*Assessment of MIC determination and Biofilm formation in the presence of antihuman DPP IV drugs*

Minimum Inhibitory Concentration determination of the AHD drugs did not show a visible growth inhibition in the concentration range studied (4 – 2048 µg/mL). A crystal violet method of biofilm determination on polystyrene 96-well plates showed that in the presence of sucrose, *S. mutans* sessile growth was not affected by any of the tested drugs, whereas all three AHD drugs tested inhibited biofilm formation in the presence of glucose, albeit with different potency (Fig. 1A). The $EC_{50}$ of each drug was determined. Results are summarized in Table 1 (in the case of sitagliptin the data point at 2048 µg/mL was not considered for fitting). The $EC_{50}$ values of all the drugs fell within the range of 128 - 512µg/mL. An ANOVA test determined that there was not a significant difference in the $EC_{50}$ among the different gliptins (F-ratio = 1.26, P = 0.328). In particular, at concentrations >128 µg/mL of saxagliptin, a 50% reduction of biofilm formation was found. Vildagliptin exerted higher inhibition of biofilm formation at concentrations ≥ 256 µg/mL. Sitagliptin demonstrated at least 50% of sessile growth inhibition at 256 µg/mL, albeit with a substantial increase observed at 2048 µg/mL as shown in Fig. 1A. Two sample comparisons of the difference in effect between saxagliptin and vildagliptin, as well as saxagliptin and sitagliptin, were significant (p = 0.023, n = 8, non – parametric Kolmogorov-Smirnov test, 95% C.I). While saxagliptin exhibited a more consistent inhibition pattern at concentrations ≥ 64 µg/mL, sitagliptin gave a sudden drop till saturation at 256-1024 µg/mL (Supplementary Fig. S1), as confirmed by the lower $EC_{50}$ value (Table 1). In the case of saxagliptin and sitagliptin, the F-test (ANOVA) showed that there was a statistically significant difference between the means at each concentration ($p_{saxagliptin}$ = 0.0013, $p_{sitagliptin}$ = 0.0089).To determine which means are significantly different from which other and to analyse the difference

bioRxiv preprint doi: https://doi.org/10.1101/157503; this version posted June 29, 2017. The copyright holder for this preprint (which was not certified by peer review) is the author/funder. All rights reserved. No reuse allowed without permission.

in effect at various concentrations, a multiple sample pairwise comparison of the means of the four independent measurements of biofilm formation at each drug concentration (number of concentrations n = 11, from 0 to 2,048 µg/mL) was performed (Supplementary Fig. S2). Means lower and higher than the $EC_{50}$ were statistically different from each other (Supplementary Fig. S2, red points). The apparent increase in biofilm formation at 2048 µg/mL of sitagliptin was found to be statistically relevant when compared with the biofilm biomass formed in presence of 128, 256, 512, and 1024 µg/mL of the drug (Supplementary Fig. S2b, cyan points). The differences observed in the presence of vildagliptin were not significant.

The viability of the cells in the planktonic phase over the formed biofilm at each concentration of drug was determined by CFU counting. *S. mutans* cells remained viable to the same extent at every concentration of drug. The colony counts at 64µg/mL - 2048µg/mL of each AHD treatment ranged between $10^9$ to $10^{10}$ CFU/mL (Supplementary Fig. S3), while the control group ($8.23 \pm 1.7 \times 10^8$CFU/mL) differed significantly by one order of magnitude from the colony counts at 2048µg/mL of each drug ($p = 0.043$, unpaired student t-test, two tailed).

*Effect of pepX deletion on S. mutans*

The stronger effect of saxagliptin on biofilm development compared to the other two AHD drugs, concomitant with a lower $K_i$ value against pure recombinant enzyme (De *et al.*, 2016), suggested a probable role of *pepX* in influencing biofilm formation by *S. mutans*. To confirm a direct function of Sm-XPDAP in the biofilm development by *S. mutans*, *pepX* was knocked out. Using primers pepX-F/R and ErypOMZ291-F/R (Table 2), deletion was confirmed by both colony PCR and subsequently by a PCR using genomic DNA as the template. Sanger sequencing of the resistance marker insertion site in the genome confirmed the correct knock-out of *pepX*

bioRxiv preprint doi: https://doi.org/10.1101/157503; this version posted June 29, 2017. The copyright holder for this preprint (which was not certified by peer review) is the author/funder. All rights reserved. No reuse allowed without permission.

(Supplementary Text 1). The stability of the allelic exchange was assured by serial passages of the mutant strain on BHI agar without the selective antibiotic and subsequent transfer on the same medium containing selective antibiotic. Replica plating experiments gave no revertants. To further verify the absence of any homologous enzyme, crude extracts from the selected deletion mutant were tested for amidolytic activity. This did not show any residual activity when compared to that of the parental (wild type) strain (data not shown). The growth rate of the *pepX* deletion mutant was comparable to that of the wild type both in BHI (data not shown) and inSDM (Supplementary Fig. S4, $P = 0.317$ by ANOVA for the fitted variable "growth rate") when optical density was measured, whereas it was lower when growth was measured as CFU (Supplementary Fig. S4, $P < 0.01$ by ANOVA for the fitted variable "growth rate"). This observation might indicate that the duplication rates in standard cultures were similar in the two strains but cell viability was decreased to some extent in the deletion mutant. Nevertheless, the *pepX* deletion mutant viable cells in the planktonic phase over the biofilm were more abundant than those of the wild type (Fig 1B, insert). This observation paralleled that obtained when biofilms were formed in the presence of AHD (Supplementary Fig. S3) and may indicate that the mutant cells are less able to aggregate or adhere to the bottom surface of the well, thus having a higher propensity to remain in suspension. Correspondingly, the biofilm forming capacity of the Δ*pepX* deletion mutant in SDM containing glucose was reduced by 70% (SD = 13.4%, n = 9, Fig. 1B), while a less substantial decrease was observed in presence of sucrose (20%; SD = 3.8%, n = 3, data not shown).

*Microscopic evaluation of adherent structured cellular organization on abiotic surface*

In order to further evaluate the influence of AHD drugs and the effect of Sm-DPP IV deficiency on the structural organization of *S. mutans* biofilms *in vitro*, CLSM of fluorescent stained cells

bioRxiv preprint doi: https://doi.org/10.1101/157503; this version posted June 29, 2017. The copyright holder for this preprint (which was not certified by peer review) is the author/funder. All rights reserved. No reuse allowed without permission.

(dead/live staining kit) was carried out. For this purpose, we decided to use saxagliptin and vildagliptin, the first for its gradual relative effect at each concentration and the second for its consideration as a reference molecule for comparing between "cyanopyrrolidides". The CLSM observation was conducted at 128 µg/mL saxagliptin and 512 µg/mL vildagliptin, which were the concentrations causing >40% biofilm inhibition (Fig. 1A). Additionally, the sudden increase in biofilm formed in the presence of 2048µg/mL sitagliptin was also investigated. At 4 hours, the adherence of wild type *S. mutans* treated with saxagliptin or vildagliptin and that of the Δ*pepX* mutant did not show any difference in respect to the untreated wild type. However, the wild type cells in the presence of saxagliptin and those of the mutant showed smaller chains and more dead cells homogenously distributed on the substratum (data not shown).

At 20 hours, the wild type demonstrated a thicker and dense homogenous layer of cell aggregation with more live cells and few void spaces, whereas the Δ*pepX* mutant exhibited a less organized thinner structure with more void spaces (Fig. 2). The visual inspection of biofilm images revealed more dead cells in the mutant, which seemed to experience more stress or alteration in the membrane integrity affecting permeation by SYTO9. Accordingly, the percentage of viability and thickness were lower in the biofilm formed by the deletion mutant with 28.5% live (green) cells and 9.6µm, respectively (Fig. 2e). Wild type counts indicated 70.4% live (green) cells and 15 µm thick biofilm mass (Fig. 2f). The effect of saxagliptin on wild type was similar to that of *pep*X deletion. At 512 µg/mL drug concentration, streptococci showed shorter dispersed chains and experienced apparent stress with higher prevalence of propidium iodide stained cells (36%) (Fig. 3e and 3f). The latter result is higher in comparison to the percentage of dead cells in the wild type (Fig. 3a-c). Vildagliptin also led to a disaggregation of the biofilm compared to the untreated control, but streptococcal chains looked healthier in

bioRxiv preprint doi: https://doi.org/10.1101/157503; this version posted June 29, 2017. The copyright holder for this preprint (which was not certified by peer review) is the author/funder. All rights reserved. No reuse allowed without permission.

comparison to the saxagliptin treated samples (Fig.3g). *S. mutans* grown in the presence of 2048µg/mL sitagliptin presented a biomass level comparable to the untreated cells. However, chains were relatively long, apparently seeming to be under stress. Visually there was no difference in aggregation and in proportion of dead cells with the control group (Fig. 3h &i).

*Comparison of cell surface properties of the wild type and ΔpepX S. mutans*

Co-aggregation and co-adhesion are integral facets of forming a stable biofilm (Kolenbrander, 2000). An assessment of the ability of *S. mutans* wild type or Δ*pepX* to co-aggregate showed a significant difference between the strains ($p < 0.01$, unpaired student t-test). The mutant aggregated 30% less that than of the wild type with a mean aggregation of 4.3%. The *pepX* mutant was also found to be less hydrophobic in independent experiments (n=2), with the wild type cells exhibiting 28 - 59% higher partitioning into toluene, though this difference in partitioning was not significant.

*Effect of environmental stress on S. mutans in absence of Sm-XPDAP*

*S. mutans* strains experience frequent ecological shifts in the oral cavity (Lemos *et al.*, 2005). An ability to tolerate acid shock and oxidative challenge allows these bacteria to colonize on the tooth surface. We hypothesized a role for *pepX* in supporting these traits. The mutant cells were found to be less resistant to acid shock than wild type cells. The cell viability of the mutant (CFU/mL) was reduced by at least three orders of magnitudes at 20 minutes post-shock, although by 30 – 40 min both wild type and the mutant showed greatly reduced numbers of colonies or no colonies (Table 3). Both the strains were equally tolerant to oxidative stress with relatively little difference even after 30 minutes (Table S1).

bioRxiv preprint doi: https://doi.org/10.1101/157503; this version posted June 29, 2017. The copyright holder for this preprint (which was not certified by peer review) is the author/funder. All rights reserved. No reuse allowed without permission.

*Differential protein expression at various conditions of in vitro biofilm assay*

In order to gain insight into the changes in the proteome of *S. mutans* either in presence of AHD molecules or in absence of Sm-DPP IV, proteomic analysis (two biological replicates) was performed using mass spectrometry. Considering the high amount of biofilm biomass required for proteome analysis in parallel to undergoing investigation of the observed effect of AHD molecules, the analyses were performed at 128 µg/mL of saxagliptin and sitagliptin. Vildagliptin was exempted from the study due to its limited effect as observed by CLSM, whereas use of 2048 µg/mL of sitagliptin was not feasible owing to the high amounts of pure molecule required.

The proteomic analysis for differentially expressed proteins confirmed the absence of PepX in the Δ*pepX* mutant. Using relatively stringent criteria for protein identification (>1 peptide identified per protein in each biological replicate) only 9 proteins were found to be more abundant in the wild type compared to the Δ*pepX* mutant (Supplementary Table S2) and no proteins were more abundant in the mutant compared to wild type. Notably the differentially expressed proteins included the Cell Surface Antigen I/II, a well characterised adhesion protein of *S. mutans* (Jenkinson and Demuth, 1997). Three of these 9 proteins were also noted to be amino acid t-RNA ligases. Comparison of control and sitagliptin-treated biofilms identified 6 proteins as more abundant in the controls and 26 as more abundant in the drug-treated cells. Likewise, comparison of control and saxagliptin-treated biofilms identified 6 proteins as more abundant in the controls (including three glycosyltransferases and levansucrase, which may affect biofilm matrix formation) and 23 as more abundant in the drug-treated cells. Two of the glycosyltransferases (SMU.910 and SMU.1005) upregulated in the controls compared to saxagliptin-treated biofilms were upregulated in the sitagliptin-treated biofilms, suggested drug specific responses that may affect biofilm remodelling. Of 49 proteins differentially expressed in

bioRxiv preprint doi: https://doi.org/10.1101/157503; this version posted June 29, 2017. The copyright holder for this preprint (which was not certified by peer review) is the author/funder. All rights reserved. No reuse allowed without permission.

either drug treatment, 12 were noted to be consistently altered in both (Supplementary Table S2). These were primarily proteins involved in protein synthesis (n = 4) or various metabolic paths (n = 7).

## Discussion

The AHD drugs used in this study are highly selective human DPP IV inhibitors (Wang *et al.*, 2012). Recent work on *in vitro* inhibition of Sm-DPP IV by gliptins has led us to hypothesize their effects on *S. mutans*, notably a role of Sm-DPP IV in regulating the behaviour of the bacterium, even though the drugs may have multiple enzyme targets. The *ex vivo* assays using these gliptins showed a notable inhibition of *S. mutans* biofilm formation. It could be speculated that this will lead to an impaired streptococcal activity in the oral cavity of diabetic patients on these medications, subject to excretion of these drugs in saliva. Saxagliptin and vildagliptin have been found to possess 50% and >90% oral bioavailability, respectively (Boulton *et al.*, 2013; Villhauer *et al.*, 2003), while saxagliptin has also been reported in the salivary glands tissue (Fred, 2009). Sitagliptin, which is quite effective against biofilm formation and classified as a high intestinal permeability and low protein binding drug, can be detected in saliva (AUC 592 ng/mL×hr) (Idkaidek & Arafat, 2012). This may suggest the possibility of excretion of the other two AHD drugs in saliva. Furthermore, our results may suggest that systemic prevalence of these drugs in prescribed users may help in averting *S. mutans* invasiveness. In this study, the basic methodology of the crystal violet procedure was not changed to keep the experimental system as simplified as possible. The replacement of the glucose carbon source with sucrose was sufficient to significantly neutralise the effects on biofilm formation in minimal medium, indicating that changes in variables are likely to mask inhibition by tested drugs. Once the fine mechanism of

bioRxiv preprint doi: https://doi.org/10.1101/157503; this version posted June 29, 2017. The copyright holder for this preprint (which was not certified by peer review) is the author/funder. All rights reserved. No reuse allowed without permission.

gliptin action in *S. mutans* has been unravelled, it will be of great interest to see how some variations in the experimental approach aimed at better mimicking the *in vivo* environment, such as addition of saliva, could modulate drug activity.

In view of the differential cell physiology in sessile form compared to planktonic phase, the very high MIC for AHD drugs was considered inconsequential (Shemesh *et al.*, 2007). As biofilm formation is an important virulence determinant in *S. mutans* more attention was paid to this aspect. To visualize the morphological and textural characteristics of *S. mutans* biofilm cells under the influence of the drugs and to confirm the observations of biofilm assay, CLSM studies were performed. Previous reports have shown that an alteration in SYTO9 staining of bacterial cells under cellular stress, due to decreased membrane permeability or reduced binding sites for the stain caused by degradation of RNA and DNA in stressed cells (Boulos *et al.*, 1999). On the other hand, propidium iodide was considered to poorly discriminate starving but surviving cells of *Escherichia coli* or *Salmonella typhimurium*, due to minimal damage of the cell membrane that may block the permeation of this dye. This may support our observation that *S. mutans* grown in the presence of AHD drugs showed clearly red cells compared to blurred green chains on the same field and magnification (López-Amorós *et al.*, 1995).

The indication that direct action of the AHD drugs on biofilm growth could be exerted through Sm-DPP IV inhibition would come from an expected similar phenotypic behaviour by the *pepX* isogenic mutant of *S. mutans* UA159. Indeed, the biofilm biomass by the *pepX* mutant was far less abundant than that formed by the wild type. This endpoint effect might be due to a reduced ability to aggregate during the first phases of biofilm formation as shown by the lower ability of the mutant to self-aggregate and its propensity to remain in suspension (planktonic state). The last behaviour was observed also upon treatment with AHD. The visible effect on biofilm

bioRxiv preprint doi: https://doi.org/10.1101/157503; this version posted June 29, 2017. The copyright holder for this preprint (which was not certified by peer review) is the author/funder. All rights reserved. No reuse allowed without permission.

formation by the mutant strain in glucose under CLSM was nearly similar to that observed in cells treated with 512 µg/mL saxagliptin. In contrast to the other AHD drugs, a sudden increase in attached biofilm was observed in presence of 2048µg/mL sitagliptin, which can likely be best explained by an increased stress response. Interestingly, there was complete inhibition of growth at the subsequent higher concentration of sitagliptin (Supplementary Fig. S5). A similar differential response to varying concentrations of the antibiotic lincomycin has also been reported in *Streptococcus pyogenes* (Malke *et al.*, 1981), albeit the mechanism of action has not been explained yet.

In this study a preliminary attempt was made to identify plausible role of PepX in modulating the proteome and investigate the site of action of AHD drugs in *S. mutans* through whole cell proteome analysis. Surprisingly, relatively few differentially expressed proteins were consistently detected. Indeed, of 56 differentially expressed proteins identified, disappointingly no single protein was consistently identified as affected in both drug treatments and the Δ*pepX* mutant. Sitagliptin treatment and the *pepX* deletion both affected the expression of valine and proline amino acid tRNA ligases, which may reflect perturbation of cytoplasmic amino acid pools and consequently an overall stress as observed under CLSM. Although several other tRNA ligases were found to be differentially regulated, these two were consistently found in each of the replicate experiments. The alteration of the level of cell surface antigen I/II (Okahashi *et al.*, 1989) was of much interest, and this may correlate with the reduced hydrophobicity and biofilm formation exhibited by the mutant. The 12 proteins that were differentially expressed in response to both drug treatments were noted to include enolase (SMU.1247), which can be a moonlighting surface-associated protein in *S. mutans* (Ge *et al.*, 2004), and acetate kinase (SMU.1978), which participates in the Pta-Ack pathway that can influence biofilm formation. The stress response

bioRxiv preprint doi: https://doi.org/10.1101/157503; this version posted June 29, 2017. The copyright holder for this preprint (which was not certified by peer review) is the author/funder. All rights reserved. No reuse allowed without permission.

chaperone GroEL (SMU.154) was more abundant following treatment with either drug, as has been observed previously in mutants with perturbed biofilm formation, whilst decreased levels of GroEL have also been linked to impaired biofilm formation (Lemos *et al.*, 2007; Matsumi *et al.*, 2015). Changes in levels of SMU.1978 and SMU.154 may thus be part of an adaptive mechanism to compensate for biofilm perturbation due to drug treatment. Alternatively, a high level of SMU.1978 may indicate the preference of *S. mutans* to participate in the Pta-Ack pathway generating high pools of ATP (formed during conversion of acetyl phosphate to acetate) by the treated stressed cells (Kim *et al.*, 2015)

In conclusion, through this work we were able to establish a potential role of *pepX* in sucrose independent biofilm development and acid tolerance of *S. mutans* and moved a step forward in identifying moieties which may be effective in developing novel Sm-DPP IV inhibitors. We have also tried to demonstrate the likely effect of AHD drugs on bacteria, as a proof of the concept that many regularly used drugs may exert some sort of side activity against microbes transiently or permanently inhabiting human body. Future studies are focused in searching or synthesizing molecules targeting Sm-DPP IV that may be applicable as new anti-caries agent. Further studies to identify the consequences of AHD drug treatments and/or *pepX* deletion in *S. mutans* will likely require a more exhaustive proteomic analysis, combined with metabolomics and transcriptomics.

**Acknowledgement**

We acknowledge Prof. Giovanni Di Bonaventura and Prof. Simone Guarnieri at Università "G. d'Annunzio" Chieti-Pescara for their help in CLSM studies. This work was supported by a Grant from MIUR-ITALY - PRIN project 2009 no. 2009P5EKH4_003 (to G.L.) and by the University of Camerino grant no.FPA00057 (to V.L.A.).

bioRxiv preprint doi: https://doi.org/10.1101/157503; this version posted June 29, 2017. The copyright holder for this preprint (which was not certified by peer review) is the author/funder. All rights reserved. No reuse allowed without permission.

## Conflicts of Interests

The authors declare no conflicts of interest.

bioRxiv preprint doi: https://doi.org/10.1101/157503; this version posted June 29, 2017. The copyright holder for this preprint (which was not certified by peer review) is the author/funder. All rights reserved. No reuse allowed without permission.

## References

**Ahn, S.-J., Ahn, S.-J., Browngardt, C. M. & Burne, R. a. (2009).** Changes in biochemical and phenotypic properties of Streptococcus mutans during growth with aeration. *Appl Environ Microbiol* **75**, 2517–27.

**Ahn, S. J., Ahn, S. J., Wen, Z. T., Brady, L. J. & Burne, R. A. (2008).** Characteristics of biofilm formation by Streptococcus mutans in the presence of saliva. *Infect Immun* **76**, 4259–68.

**Ahn, S. J., Cho, E. J., Kim, H. J., Park, S. N., Lim, Y. K. & Kook, J. K. (2012).** The antimicrobial effects of deglycyrrhizinated licorice root extract on Streptococcus mutans UA159 in both planktonic and biofilm cultures. *Anaerobe* **18**, 590–6. Elsevier Ltd.

**Ajdić, D., McShan, W. M., McLaughlin, R. E., Savić, G., Chang, J., Carson, M. B., Primeaux, C., Tian, R., Kenton, S. & other authors. (2002).** Genome sequence of Streptococcus mutans UA159, a cariogenic dental pathogen. *Proc Natl Acad Sci U S A* **99**, 14434–9.

**Bagramian, R. A., Garcia-Godoy, F. & Volpe, A. R. (2009).** The global increase in dental caries. A pending public health crisis. *Am J Dent* **22**, 3–8.

**Boulos, L., Prevost, M., Barbeau, B., Coallier, J. & Desjardins, R. (1999).** Methods LIVE / DEAD ® Bac Light E□: application of a new rapid staining method for direct enumeration of viable and total bacteria in drinking water **37**, 77–86.

**Boulton, D. W., Kasichayanula, S., Keung, C. F. A., Arnold, M. E., Christopher, L. J., Xu, X. S. & Lacreta, F. (2013).** Simultaneous oral therapeutic and intravenous $^{14}$C-microdoses to determine the absolute oral bioavailability of saxagliptin and dapagliflozin. *Br J Clin Pharmacol* **75**, 763–8.

**CLSI. (2011).** *Performance Standards for Antimicrobial Susceptibility Testing; Twenty First Informational Supplement*. Clinical and Laboratory Standards Institute.

**Cowman, R. A. & Baron, S. S. (1997).** Pathway for Uptake and Degradation of X-Prolyl Tripeptides in Streptococcus mutans VA-29R and Streptococcus sanguis ATCC 10556. *J Dent Res* **76**, 1477–1484.

**Cowman, R., Fitzgerald, R., Perrella, M. & Cornell, A. (1977).** Human saliva as a nitrogen source for oral streptococci. *Caries Res* **11**, 1–8.

**Cowman, R. A. & Baron, S. S. (1990, December).** Influence of hydrophobicity on oligopeptide utilization by oral streptococci. *J Dent Res*.

**Cowman, R. A. & Baron, S. S. (1993).** Comparison of aminopeptidase activities in four strains of mutans group oral streptococci. *Infect Immun* **61**, 182–6.

**Cowman, R. A., Perrella, M. M. & Fitzgerald, R. J. (1975).** Caseinolytic and glyoprotein hydrolase activity of Streptococcus mutans. *J Dent Res* **55**, 391–9.

**De, A., Lupidi, G., Petrelli, D. & Vitali, L. A. (2016).** Molecular cloning and biochemical characterization of Xaa-Pro dipeptidyl-peptidase from Streptococcus mutans and its inhibition by anti-human DPP IV drugs. *FEMS Microbiol Lett* **363**, fnw066. The Oxford University Press.

bioRxiv preprint doi: https://doi.org/10.1101/157503; this version posted June 29, 2017. The copyright holder for this preprint (which was not certified by peer review) is the author/funder. All rights reserved. No reuse allowed without permission.

**Fred, A. (2009).** Pharmacokinetis tabulated summary. *NDA no 22-350*.

**Ge, J., Catt, D. M. & Gregory, R. L. (2004).** Streptococcus mutans surface alpha-enolase binds salivary mucin MG2 and human plasminogen. *Infect Immun* **72**, 6748–52.

**Ge, J., Feng, Y., Ji, H., Zhang, H., Zheng, F., Wang, C., Yin, Z., Pan, X. & Tang, J. (2009).** Inactivation of dipeptidyl peptidase IV attenuates the virulence of Streptococcus suis serotype 2 that causes streptococcal toxic shock syndrome. *Curr Microbiol* **59**, 248–55.

**Goldstein, J. M., Banbula, A., Kordula, T. & Mayo, J. A. (2001).** Novel Extracellular x-Prolyl Dipeptidyl-Peptidase ( DPP ) from Streptococcus gordonii FSS2□: an Emerging Subfamily of Viridans Streptococcal x-Prolyl DPPs. *Infect Immun* **69**, 5494–5501.

**Green, B. D., Flatt, P. R. & Bailey, C. J. (2006).** Dipeptidyl peptidase IV (DPP IV) inhibitors: A newly emerging drug class for the treatment of type 2 diabetes. *Diab Vasc Dis Res* **3**, 159–65.

**Idkaidek, N. & Arafat, T. (2012).** Saliva versus plasma pharmacokinetics: theory and application of a salivary excretion classification system. *Mol Pharm* **9**, 2358–63. American Chemical Society.

**Kim, J. N., Ahn, S.-J. & Burne, R. A. (2015).** Genetics and Physiology of Acetate Metabolism by the Pta-Ack Pathway of Streptococcus mutans. *Appl Environ Microbiol* **81**, 5015–5025 (M. Kivisaar, Ed.).

**King, H., Aubert, R. & Herman, W. (1998).** Global burden of diabetes 1995–2025. *Diabetes Care* **21**, 1414–1431.

**Kolenbrander, P. E. (2000).** Oral Microbial Communities: Biofilms, Interactions, and Genetic Systems 1. *Annu Rev Microbiol* **54**, 413–437.

**Lau, P. C. Y., Sung, C. K., Lee, J. H., Morrison, D. a & Cvitkovitch, D. G. (2002).** PCR ligation mutagenesis in transformable streptococci: application and efficiency. *J Microbiol Methods* **49**, 193–205.

**Lemos, J. A., Luzardo, Y. & Burne, R. A. (2007).** Physiologic effects of forced down-regulation of dnaK and groEL expression in Streptococcus mutans. *J Bacteriol* **189**, 1582–8. American Society for Microbiology.

**Lemos, J. A. C., Abranches, J. & Burne, R. A. (2005).** Responses of cariogenic streptococci to environmental stresses. *Curr Issues Mol Biol* **7**, 95–107.

**López-Amorós, R., Comas, J. & Vives-Rego, J. (1995).** Flow cytometric assessment of Escherichia coli and Salmonella typhimurium starvation-survival in seawater using rhodamine 123, propidium iodide, and oxonol. *Appl Environ Microbiol* **61**, 2521–6.

**Malke, H., Reichardt, W., Hartmann, M. & Walter, F. (1981).** Genetic study of plasmid-associated zonal resistance to lincomycin in Streptococcus pyogenes. *Antimicrob Agents Chemother* **19**, 91–100.

**Matsumi, Y., Fujita, K., Takashima, Y., Yanagida, K., Morikawa, Y. & Matsumoto-Nakano, M. (2015).** Contribution of glucan-binding protein A to firm and stable biofilm formation by *Streptococcus mutans*. *Mol Oral Microbiol* **30**, 217–226.

**Nance, W. C., Dowd, S. E., Samarian, D., Chludzinski, J., Delli, J., Battista, J. & Rickard, A. H. (2013).** A high-throughput microfluidic dental plaque biofilm system to visualize and

bioRxiv preprint doi: https://doi.org/10.1101/157503; this version posted June 29, 2017. The copyright holder for this preprint (which was not certified by peer review) is the author/funder. All rights reserved. No reuse allowed without permission.

quantify the effect of antimicrobials. *J Antimicrob Chemother* **68**, 2550–60.

**Okahashi, N., Sasakawa, C., Yoshikawa, M., Hamada, S. & Koga, T. (1989).** Molecular characterization of a surface protein antigen gene from serotype c Streptococcus mutans , implicated in dental caries. *Mol Microbiol* **3**, 673–678.

**Petersen, F. C. & Scheie, A. A. (2000).** Genetic transformation in Streptococcus mutans requires a peptide secretion-like apparatus. *Oral Microbiol Immunol* **15**, 329–34.

**van der Ploeg, J. R. (2008).** Characterization of Streptococcus gordonii prophage PH15: complete genome sequence and functional analysis of phage-encoded integrase and endolysin. *Microbiology* **154**, 2970–8.

**Rosengren, L. & Winblad, B. (1976).** Proteolytic activity of Streptococcus mutans (GS-5). *Oral Surg Oral Med Oral Pathol* **42**, 801–9.

**Selwitz, R. H., Ismail, A. I. & Pitts, N. B. (2007).** Dental caries. *Lancet* **369**, 51–9.

**Shemesh, M., Tam, A. & Steinberg, D. (2007).** Expression of biofilm-associated genes of Streptococcus mutans in response to glucose and sucrose. *J Med Microbiol* **56**, 1528–35.

**da Silva, B. R., de Freitas, V. A. A., Carneiro, V. A., Arruda, F. V. S., Lorenzón, E. N., de Aguiar, A. S. W., Cilli, E. M., Cavada, B. S. & Teixeira, E. H. (2013).** Antimicrobial activity of the synthetic peptide Lys-a1 against oral streptococci. *Peptides* **42**, 78–83.

**Smith, K. & Beighton, D. (1986).** The effects of the availability of diet on the levels of exoglycosidases in the supragingival plaque of macaque monkeys. *J Dent Res* **65**, 1349–52.

**Villhauer, E. B., Brinkman, J. a., Naderi, G. B., Burkey, B. F., Dunning, B. E., Prasad, K., Mangold, B. L., Russell, M. E. & Hughes, T. E. (2003).** 1-[[(3-Hydroxy-1-adamantyl)amino]acetyl]-2-cyano-(S)-pyrrolidine: A potent, selective, and orally bioavailable dipeptidyl peptidase IV inhibitor with antihyperglycemic properties. *J Med Chem* **46**, 2774–89.

**Wang, A., Dorso, C., Kopcho, L., Locke, G., Langish, R., Harstad, E., Shipkova, P., Marcinkeviciene, J., Hamann, L. & Kirby, M. S. (2012).** Potency, selectivity and prolonged binding of saxagliptin to DPP4: maintenance of DPP4 inhibition by saxagliptin in vitro and ex vivo when compared to a rapidly-dissociating DPP4 inhibitor. *BMC Pharmacol* **12**, 2. BioMed Central Ltd.

**Yagishita, H., Kumagai, Y., Konishi, K., Takahashi, Y., Aoba, T. & Yoshikawa, M. (2001).** Histopathological studies on virulence of dipeptidyl aminopeptidase IV (DPPIV) of Porphyromonas gingivalis in a mouse abscess model: use of a DPPIV-deficient mutant. *Infect Immun* **69**, 7159–61.

bioRxiv preprint doi: https://doi.org/10.1101/157503; this version posted June 29, 2017. The copyright holder for this preprint (which was not certified by peer review) is the author/funder. All rights reserved. No reuse allowed without permission.

## Figure Legends

Fig.1.Quantification of biofilm formed by *S. mutans* in the presence of AHD drugs and of biofilm formed by a *pepX* deletion mutant. A. Histogram represents mean % biofilm formation in minimal medium containing 0-2048 µg/mL AHD drugs (n = 4, with duplicates within each independent experiment), B. Comparison of biofilm formation between Δ*pepX* (in black) and wild type (in white) *S. mutans* in minimal medium containing glucose (n = 3, performed in triplicates within each independent experiment). Error bars represent standard deviation (p-value <0.001). Insert: viable cells count (expressed as CFU/mL) in the planktonic phase over the biofilm formed in SDM containing glucose.

Fig. 2. CLSM comparative study of biofilms formed by the Δ*pepX* mutant and wild type *S. mutans* after 20 h. (a) Δ *pepX* mutant ($1^{st}$ field), (b) Δ *pepX* mutant ($2^{nd}$ field), (c) wild type ($1^{st}$ field), (d) wild type ($2^{nd}$ field), (e) z-axis representation of biofilm formed by Δ *pepX* mutant, (f) z-axis representation of biofilm formed by wild type.

Fig. 3. CLSM images of *S. mutans* untreated controls and treated with AHD drugs. (a) Untreated (1st field), (b) Untreated (2nd field), (c) Untreated (3rd field), (d) 128µg/mL saxagliptin treated, (e) 512µg/mL saxagliptin treated (1st field), (f) 512µg/mL saxagliptin treated (2nd field), (g) 512µg/mL vildagliptin treated, (h) 2048µg/mL sitagliptin treated (1st field), (i) 2048µg/mL sitagliptin treated (2nd field).

bioRxiv preprint doi: https://doi.org/10.1101/157503; this version posted June 29, 2017. The copyright holder for this preprint (which was not certified by peer review) is the author/funder. All rights reserved. No reuse allowed without permission.

## Tables

**Table 1. $EC_{50}$ values for each drug.** Mean concentration of drug producing 50% reduction in biofilm formation ($EC_{50}$) was calculated from four independent replicates. Standard deviations (SD) were also determined.

| **Drug** | **$EC_{50}$± SD (µg/mL)** |
|---|---|
| Saxagliptin | **205 ± 71** |
| Vildagliptin | **280 ± 150** |
| Sitagliptin | **167 ± 67** |

Table 2. **Oligonucleotide DNA primers used in the present work.**

| Name | Primer sequence |
|---|---|
| Ery pOMZ291-F | 5’- TAATCCATGGCACAAGTGATTTGTGATTGTTG-3’ |
| Ery pOMZ291-R | 5’- TAATGAGCTCTAGGCGCTAGGGACCTCTTT-3’ |
| pepX-Up-F | 5’- ATTGTCTTTTGCGTAGCATCTT-3’ |
| pepX-Up-R | 5’- TAATGAGCTCAAACCGTTCGTGATAACAGC-3’ |
| pepX-Dn-F | 5’- TAATCCATGGAGGTCGCTAAGTTTGCTTTATTG-3’ |
| pepX-Dn-R | 5’- TCCACAGCTGAGATAGTAGAGAATG-3’ |



bioRxiv preprint doi: https://doi.org/10.1101/157503; this version posted June 29, 2017. The copyright holder for this preprint (which was not certified by peer review) is the author/funder. All rights reserved. No reuse allowed without permission.

bioRxiv preprint doi: https://doi.org/10.1101/157503; this version posted June 29, 2017. The copyright holder for this preprint (which was not certified by peer review) is the author/funder. All rights reserved. No reuse allowed without permission.

Table 3.**Cell counts (CFU/mL) after acid shock.** Acid shock assay was performed in three independent experiments (indicated by the numbering after **Δ*pepX***) with duplicate platings within each experiment.

| ***S. mutans*** | 0 | 10 | 20 | 30 | 35 | 40 |
|---|---|---|---|---|---|---|
| **Wild type** | 2.5E+08 | 5.4E+05 | 2.2E+06 | 2.6E+02 | - | 0.0E+00 |
| **Δ*pepX*1** | 2.2E+08 | 4.2E+05 | 0.0E+00 | - | 0.0E+00 | - |
| **Δ*pepX*2** | 5.0E+08 | 1.6E+06 | 6.7E+03 | - | 0.0E+00 | - |
| **Δ*pepX*3** | 1.7E+09 | 2.4E+06 | 6.5E+03 | - | 5.1E+02 | - |

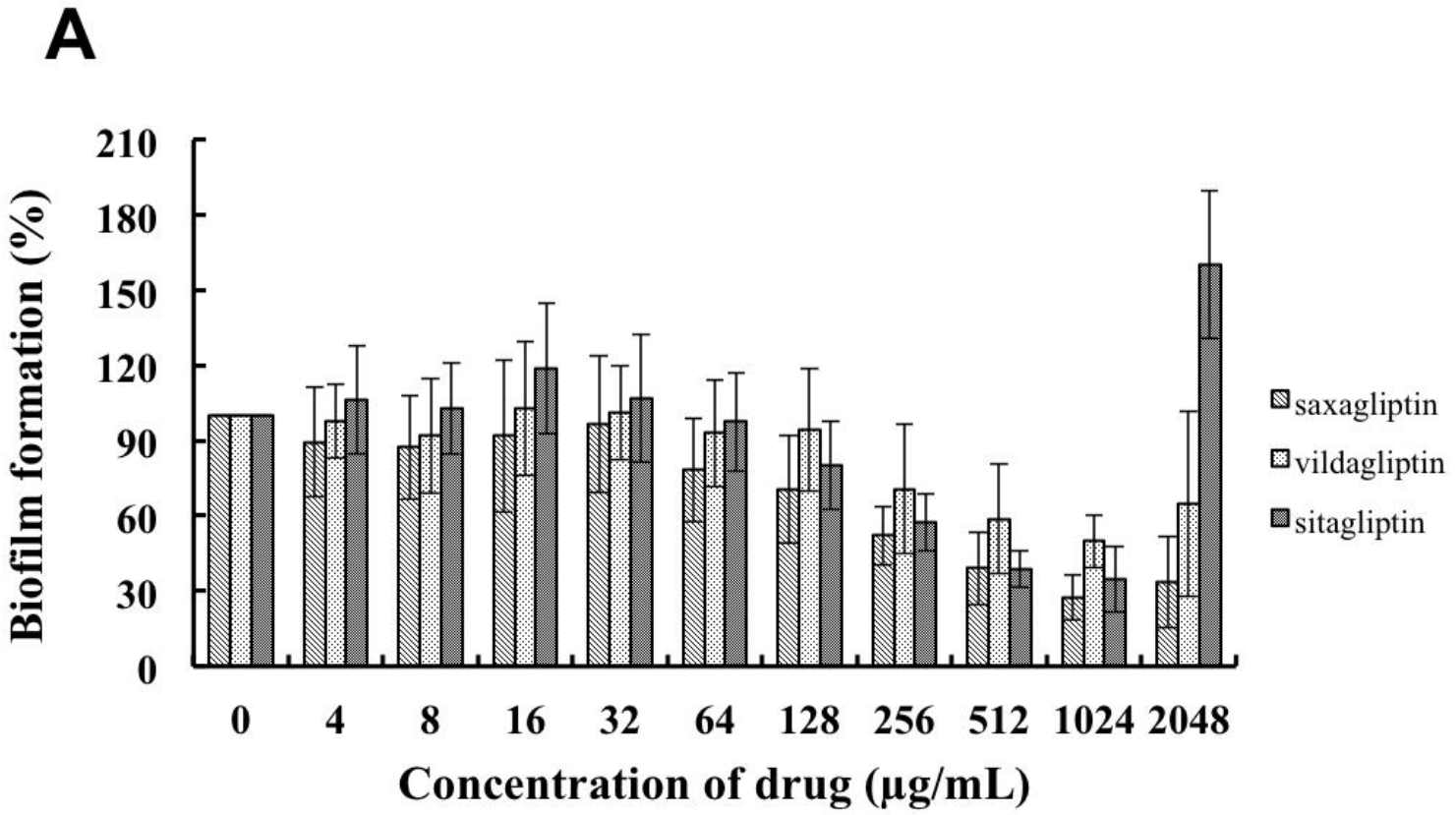
A
Biofilm formation (%)
210
180
150
120
90
60
30
0
0
4
8
16
32
64
128
256
512
1024
2048
Concentration of drug (μg/mL)
saxagliptin
vildagliptin
sitagliptin

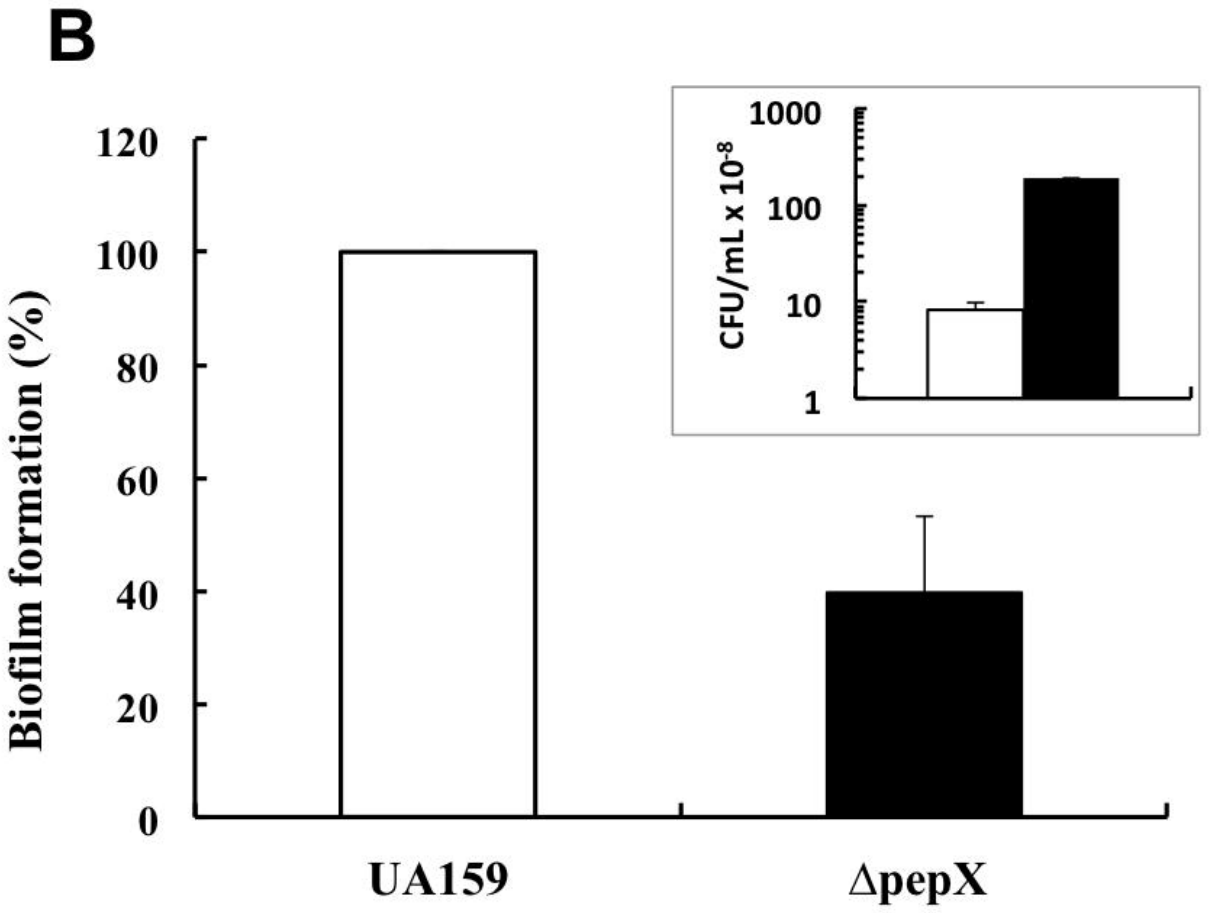
B
Biofilm formation (%)
120
100
80
60
40
20
0
UA159
ΔpepX
CFU/mL x 10-8
1000
100
10
1

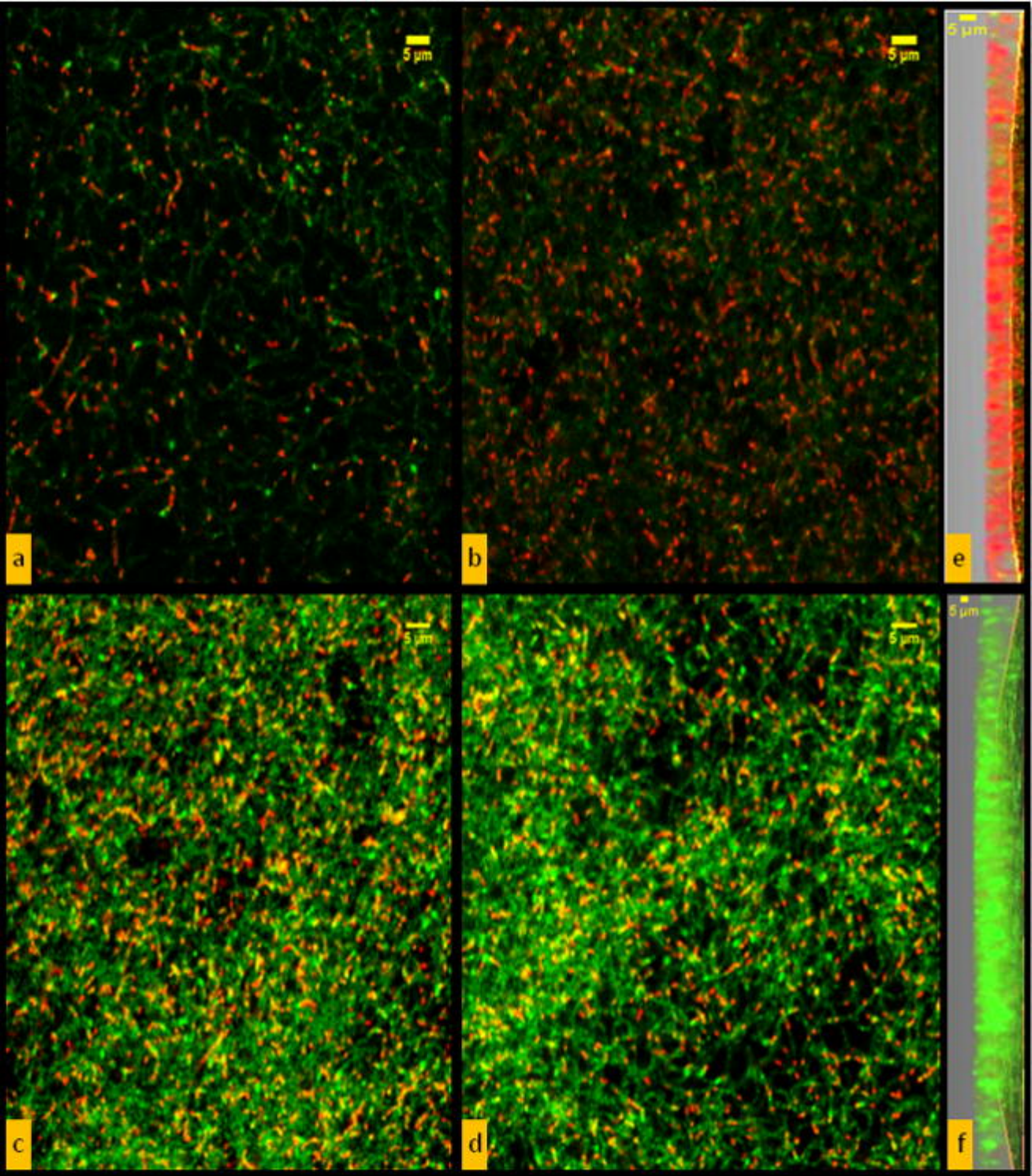
5 µm
5 µm
5 µm
a
b
e
5 µm
5 µm
5 µm
c
d
f

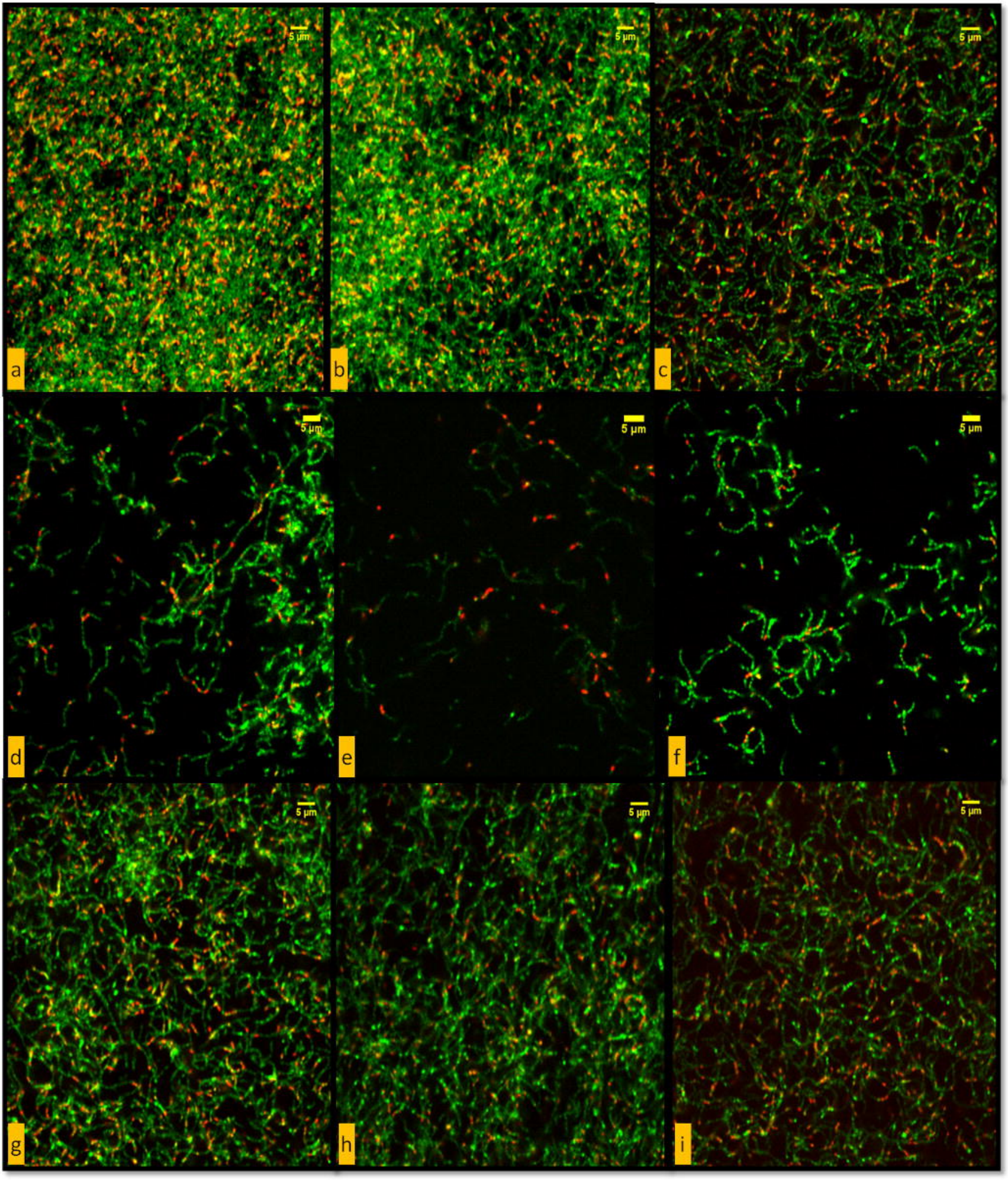
5 µm
a
5 µm
b
5 µm
c
5 µm
d
5 µm
e
5 µm
f
5 µm
g
5 µm
h
5 µm
i